Mitochondrion 13 (2013) 749–754

Contents lists available at ScienceDirect

Mitochondrion

journal homepage: www.elsevier.com/locate/mito

A novel familial case of diffuse leukodystrophy related to *NDUFV1* compound heterozygous mutations

Oscar Ortega-Recalde [a,1], Dora Janeth Fonseca [a,b,1], Liliana Catherine Patiño [a], Juan Jaime Atuesta [c], Carolina Rivera-Nieto [a], Carlos Martín Restrepo [a,b], Heidi Eliana Mateus [a], Marjo S. van der Knaap [d], Paul Laissue [a,b,*]

[a] Unidad de Genética, Escuela de Medicina y Ciencias de la Salud, Universidad del Rosario, Bogotá, Colombia
[b] Genética Molecular de Colombia, Departamento de Genética Molecular, Bogotá, Colombia
[c] Centro Dermatológico Federico Lleras Acosta, Bogotá, Colombia
[d] Department of Child Neurology, VU University Medical Center, Amsterdam, The Netherlands

ARTICLE INFO

Article history:
Received 13 December 2012
Received in revised form 25 March 2013
Accepted 27 March 2013
Available online 4 April 2013

Keywords:
Mitochondrial disease
Diffuse leukodystrophy
NDUFV1 mutations
Genetics

ABSTRACT

NDUFV1 mutations have been related to encephalopathic phenotypes due to mitochondrial energy metabolism disturbances. In this study, we report two siblings affected by a diffuse leukodystrophy, who carry the *NDUFV1* c.1156C>T (p.Arg386Cys) missense mutation and a novel 42-bp deletion. Bioinformatic and molecular analysis indicated that this deletion lead to the synthesis of mRNA molecules carrying a premature stop codon, which might be degraded by the nonsense-mediated decay system. Our results add information on the molecular basis and the phenotypic features of mitochondrial disease caused by *NDUFV1* mutations.

1. Introduction

Mitochondrial respiratory chain disorders (MD) are a group of phenotypically heterogeneous pathologies characterized by energy metabolism disturbances. Clinical manifestations include hepatopathy, cardiomyopathy, lactic acidosis, leukoencephalopathy and Leigh syndrome. MD are among the most frequent inherited neurological disorders (Skladal et al., 2003; Thorburn, 2004). They are caused by both nuclear and mitochondrial DNA mutations, especially in genes encoding Complex I (CI) proteins (Pagniez-Mammeri et al., 2012). CI, also named nicotinamide adenine dinucleotide (NADH): ubiquinone oxidoreductase, is a multiprotein complex assembled from more than 40 subunits, encoded by nuclear and mitochondrial DNA (Brandt, 2006). The CI central catalytic core is composed by 14 functional subunits forming three major modules (named N, P and Q) (Brandt, 2006; Pagniez-Mammeri et al., 2012). Briefly, the N module (input module) oxidizes NADH, the P module translocates protons across the membrane and the Q module (output module) reduces ubiquinone. The NADH dehydrogenase (ubiquinone) flavoprotein 1 (NDUFV1) subunit is a part of the N module and binds to the flavin mononucleotide, a structure that transfers electrons from NADH to iron-sulfur clusters. Up to now, sixteen pathogenic *NDUFV1* mutations have been reported in patients displaying encephalopathic phenotypes (Benit et al., 2001; Breningstall et al., 2008; Bugiani et al., 2004; Calvo et al., 2010; Koene et al., 2012; Laugel et al., 2007; Moran et al., 2010; Schuelke et al., 1999; Vilain et al., 2012; Zafeiriou et al., 2008). However, no genotype–phenotype correlations have been clearly identified. This might be due to the structural and functional complexity of CI and to the difficulty to perform functional tests.

In this study, we report two siblings affected by a diffuse leukodystrophy, who carry a previously reported point mutation (p.Arg386Cys) and a novel 42 bp deletion encompassing the intron 6/exon 7 junction of *NDUFV1*. Bioinformatic and molecular analysis indicated that this mutation lead to the synthesis of mRNA molecules carrying a premature stop codon, which might be degraded by the nonsense-mediated decay (NMD) system. Our results add information on the molecular basis and the phenotypic features of mitochondrial disease caused by *NDUFV1* mutations.

2. Case report

Patients and their parents attended the Genetics Unit at El Rosario University (Bogotá, Colombia). This study has been approved by the Ethical Committee at Universidad del Rosario and was conducted

Abbreviations: MD, mitochondrial respiratory chain disorders; CI, complex I; NMD, nonsense-mediated decay.

* Corresponding author at: Unidad de Genética, Escuela de Medicina y Ciencias de la Salud. Universidad del Rosario. Bogotá, Carrera 24 N° 63C-69, Bogotá, Colombia. Tel./fax: +57 1 3474570.
E-mail address: paul.laissue@urosario.edu.co (P. Laissue).

[1] Both authors contributed equally to this work.

1567-7249/$ – see front matter
http://dx.doi.org/10.1016/j.mito.2013.03.010

according to the Declaration of Helsinki Principles. Parents established a written informed consent and signed it on behalf of their sons.

Patient 1 (P1) is a 5-year-old male of Colombian origin, born after a term pregnancy of 39 weeks. Delivery was performed via cesarean section. His parents, 41 (father) and 30 (mother) years old, were healthy and not known to be consanguineous. At the age of one year he presented with psychomotor regression and irritability. At this time, clinical examination showed inability to sit, poor head control, spasticity, brisk reflexes, sustained clonus, strabismus and nystagmus. Persistent metabolic acidosis was recorded. Blood and cerebrospinal fluid biochemical investigations displayed high levels of lactate. An electroencephalogram showed paroxysmal activity in the left centroparietal region of the brain. Magnetic resonance imagery (MRI) of the brain showed prominent signal abnormalities in large regions of the cerebral white matter, which include the corpus callosum (Fig. 1). The corpus callosum was swollen. Fluid attenuated inversion recovery (FLAIR) images revealed that large areas of the white matter were rarefied and cystic. Some better preserved tissue strands were observed in these areas. The cysts were well-delineated and surrounded by a rim of abnormal but solid tissue. A rim of periventricular tissue was preserved. The basal nuclei, thalami, brain stem and cerebellum were normal. A spinal cord MRI did not show abnormalities. A magnetic resonance spectroscopy displayed high lactate levels within the abnormal white matter. At the age of 5 years slight improvement in motor abilities and language milestones was observed. However, gait instability, brisk reflexes, sustained clonus and fisting were documented. Blood lactate and pyruvate levels were normal. MRI demonstrated extensive atrophy of the white matter. The corpus callosum had become thin. FLAIR images showed that the rarefied and cystic areas had collapsed. Some small cysts were present. The lateral ventricules had become wider. The basal nuclei, the thalami, the brain stem and the cerebellum were not affected.

The P1's brother (patient 2, P2) is a 2-year-old male who developed normally until the age of 12 months. At this time, he presented with psychomotor regression, weakness, eating difficulties and laryngeal stridor. Physical examination showed poor head control, spasticity, brisk reflexes, clonus and nystagmus with divergent strabismus. Although blood lactate and pyruvate levels were normal, MRI of the brain displayed a similar pattern of abnormalities as observed in P1. Based on these features mitochondrial leukoencephalopathy was diagnosed (Schuelke et al., 1999), as can be caused by *NDUFV1* mutations (Zafeiriou et al., 2008).

3. Materials and methods

3.1. NDUFV1 molecular analysis

Genomic DNA was obtained from whole blood samples using standard procedures. The complete coding region, 10 exons of *NDUFV1* [Ensembl: ENST00000322776] was amplified in patients and their parents using 5′ and 3′ flanking oligonucleotides. Primer sequences and PCR conditions are available on request. Each amplicon was purified using shrimp alkaline phosphatase and exonuclease I, as described by the manufacturer (USB, Cleveland, Ohio, USA). Direct sequencing was performed with internal primers using an ABI 3100 sequencer (Applied Biosystems, Foster City, CA, USA). In order to avoid an inaccurate description of c.914-8G_947del mutation (see below), secondary to heterozygous insertion/deletion sequencing profiles (double peaks), intron 6 and exon 7 amplicons from P1 were cloned into a pCR4-TOPO-TA plasmid (Invitrogen) and directly sequenced. Mutation nomenclature follows den Dunnen and Antonarakis' (2000) recommendations, which were last modified on April 20, 2012 (http://www.hgvs.org). [Ensembl: ENST00000322776] sequence was used as reference to describe mutations.

A skin biopsy was performed in the mother. Trizol reagent and Pure Link RNA minikit (Life Technologies) were used to isolate total RNA. cDNA was synthesized using Superscript III Reverse Transcriptase (Life Technologies). *NDUFV1*-cDNA from the first ATG to the stop codon was amplified by standard PCR and directly sequenced with internal primers.

3.2. In silico analysis

New potential intron 6 splice donor sites generated by c.914-8G_947del mutation were studied using Augustus (http://bioinf.uni-greifswald.de/bioinf) and NetGene2 (www.cbs.dtu.dk) software (Brunak et al., 1991; Stanke et al., 2006). First, in order to establish the reliability of this approach, wild type (WT) *NDUFV1* full length exonic and intronic sequences were used to predict the complete coding sequence of the gene. Since the predicted sequence corresponded to the longest coding sequence present in public databases, we then performed identical analysis using the c.914-8G_947del mutant sequence. ClustalW (http://www.ebi.ac.uk/Tools/msa/clustalw2) software was used to align human WT, [GenBank: NP_009034.2] and mutant sequences with those from numerous species, *Mus musculus* [GenBank: NP_598427.1],

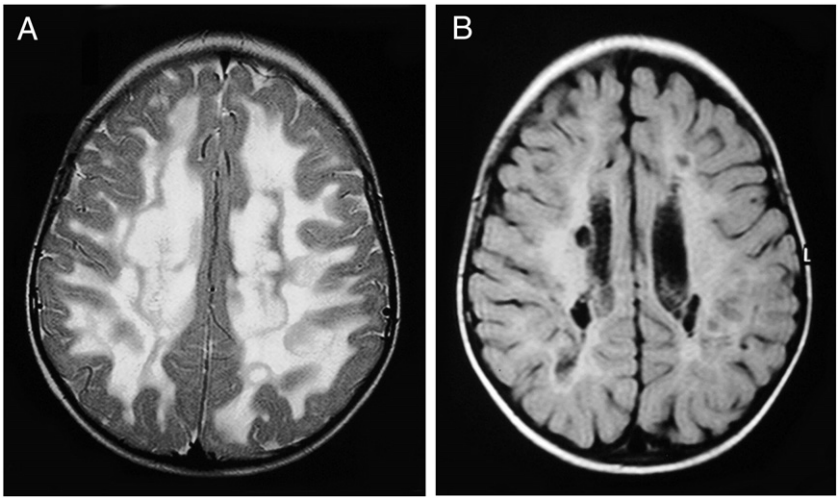

Fig. 1. MRI of P1's brain. A: T2-weighted (4645/100 [TR/TE]) and FLAIR. B: axial turbo spin-echo image showing that large areas of the white matter are rarefied and cystic, with better preserved tissue strands in the rarefied and cystic areas.

Rattus norvegicus [GenBank: NP_001006973.1], *Bos Taurus* [GenBank: NP_777233.1], *Xenopus laevis* [GenBank: NP_001080215.1] and *Dictyostelium discoideum* [GenBank: AAB03672.1]. SIFT (http://blocks.fhcrc.org/sift/SIFT.html) and PolyPhen-2 (http://genetics.bwh.harvard.edu/pph2/) software were used to study the potential deleterious effect of p.Arg386Cys aminoacid substitution.

4. Results

Exons 6-7 gel electrophoresis from patients and their mother displayed double bands, which pinpointed the presence of a heterozygous insertion/deletion (Fig. 2). Direct sequencing of the complete *NDUFV1* coding region revealed, in both patients, c.1156C>T (p.Arg386Cys), [dbSNP: rs150966634] and c.914-8G_947del heterozygous mutations (Fig. 3). The c.914-8G_947del mutation was confirmed by additional sequencing of intron 6/exon 7 amplicons, which were previously cloned in order to separate the parental alleles (Fig. 3). Patient's p.Arg386Cys and c.914-8G_947del mutations were inherited from the father and the mother, respectively. The c.914-8G_947del mutation deletes 8 nucleotides located at the end of intron 6 and 34 base pairs of the 5′ region of exon 7 (Supplementary Fig. S1). Because this deletion removes classical intron–exon splice sites, distinct transcription and translation events could be predicted by bioinformatics (Fig. 4). Thus, intron 6 might be retained, which creates an aberrant truncated protein tail of 35 residues (*Pred1*, p. Gly306Lysfs*36 mutation). This mutation might also generate the skipping of exon 7, which potentially generates a premature stop codon and an aberrant tail of 11 aminoacids (*Pred2*, p.Gly305Aspfs*12 mutation). Finally, Augustus and NetGene bioinformatics tools predicted the existence of a cryptic splice site located 34 nucleotides upstream of the c.914-8G_947del deletion, which changes GGVTGGWDNLLA to ALTMHPFGDRLG residues (positions 305 to 316) (*Pred3*). In this case, the protein sequence (which displays an identical length as compared to the WT version) might be recovered from valine at position 317. RT-PCR of *NDUFV1*-cDNA from skin expressed transcripts showed a unique band and its direct sequencing demonstrated a chromatogram profile that corresponds to the WT sequence.

In silico analysis of the p.Arg386Cys mutation revealed that it is located in a high conserved region among vertebrate and non-vertebrate species (Fig. 4). SIFT and Polyphen bioinformatics tools showed that Arg to Cys aminoacid substitution scores are compatible with a potential deleterious effect (0 and 0.999, respectively).

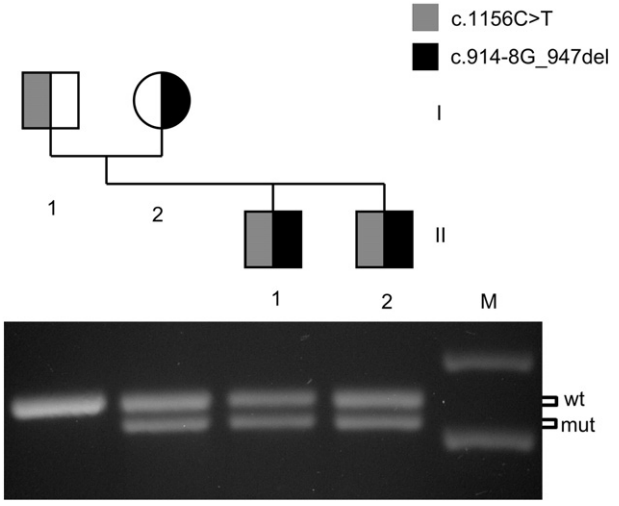

Fig. 2. Pedigree of the Colombian family affected by diffuse leucodystrophy originated from *NDUFV1* mutations. Top: the black half-filled symbols represent the c.1156C>T (p.Arg386Cys) and the gray half-filled symbols the c.914-8G_947del mutation. Bottom: Exons 6-7 gel electrophoresis which displays double bands in patients and their mother. The last lane of the gel electrophoresis corresponds to the DNA ladder (M, upper band 1000 bp, lower band 850 bp).

5. Discussion

Complex I deficiencies comprise a considerable range of medical conditions which affect distinct organs, especially those of the central nervous system (Bugiani et al., 2004). In our study, Leigh/Leigh-like syndrome diagnosis was excluded since brain MRI lacks basal ganglia, brain stem and cerebellum lesions (Lebre et al., 2011). We considered that *NDUFV1* or *NDUFS1* might be related to the phenotype since their mutations frequently originate energy metabolism disturbances associated to leukodystrophy (Janssen et al. 2006; Koene et al., 2012; Pagniez-Mammeri et al., 2012). Therefore, the first step of our approach consisted to direct sequence their coding regions. The identification of a causative mutation in *NDUFV1* avoided subsequent *NDUFS1* sequencing.

Clinically, our patients, who present the c.1156C>T (p.Arg386Cys)/c.914-8G_947del compound heterozygous mutations, are affected by a less severe phenotype than those reported in the majority of individuals carrying *NDUFV1* biallelic mutations.

Indeed, they displayed a late onset of first symptoms, have no history of epilepsy and P1 survived until the age of 5 years with a progressive improvement of motor and language skills (Table 1). Moreover, although lactate and pyruvate quantities were initially elevated, normal levels were subsequently restored. This mild phenotype resembles to that reported in patients presenting p.Arg386Cys homozygous and p.Arg257Gln/p.Ala211Val compound heterozygous mutations (Breningstall et al., 2008; Zafeiriou et al., 2008).

Recently, Vilain et al. (2012) reported two siblings affected by Leigh syndrome who presented the p.Arg386His homozygous mutation. In these patients, neurological function was severely affected since first symptoms appeared at 3.5 months of age with a rapid degradation leading to death. This considerable phenotypic variability among patients presenting Arg386 mutations might be due to intrinsic physicochemical characteristics of the interchanged aminoacids. Although Arg, Cys, and His residues have hydrophobic properties, the aromatic structure of histidine might perturb the correct function of Cys385 during the mitochondrial inner membrane electron transfer step. Indeed, it has been demonstrated that Cys379, Cys382, Cys385 and Cys425 have an essential role during Fe atoms arrangement into the NDUFV1 iron-sulfur cluster (Hirst et al., 2003; Vilain et al., 2012). Furthermore, it would be possible that the presence of two contiguous cysteines at positions 385 and 386 (as it is the case in the present study and in that reported by Breningstall et al. (2008)) preserves a minimal functionality in the proton transfer function (Breningstall et al., 2008). This might explain why p.Arg386Cys patients are affected by a mildly progressive course of the disease.

The second pathogenic mutation (c.914-8G_947del) found in our patients eliminates the intron 6/exon 7 canonical splice acceptor site. Therefore, this mutation might result in the transcription of the intron 6/exon 7 mutated allele (*Pred1*), the complete exon 7 skipping (*Pred2*) or the activation of potential cryptic splice sites (*Pred 3*) (Fig. 4). *Pred1* and *Pred2* are related to the synthesis of truncated proteins displaying aberrant tails. In this context, since the premature stop codons are potentially situated at least 50 nucleotides upstream of an exon–exon boundary, it is likely that mutant mRNAs be recognized and degraded by the NMD machinery (Nagy and Maquat, 1998). Sequence analysis of the maternal *NDUFV1*-cDNA from skin tissue supports this hypothesis as only the WT version of the gene was identified. However, it is important to note that our results do not formerly validate NMD as the pathogenic mechanism. Indeed, the lack of *NDUFV1*-mRNA transcripts in the skin tissue does not necessarily reflect the molecular behavior of mutated molecules in the brain. Furthermore, it has been demonstrated that, in distinct tissues, for a specific mutation NMD can functions differentially (Bateman et al., 2003). Our results, as those

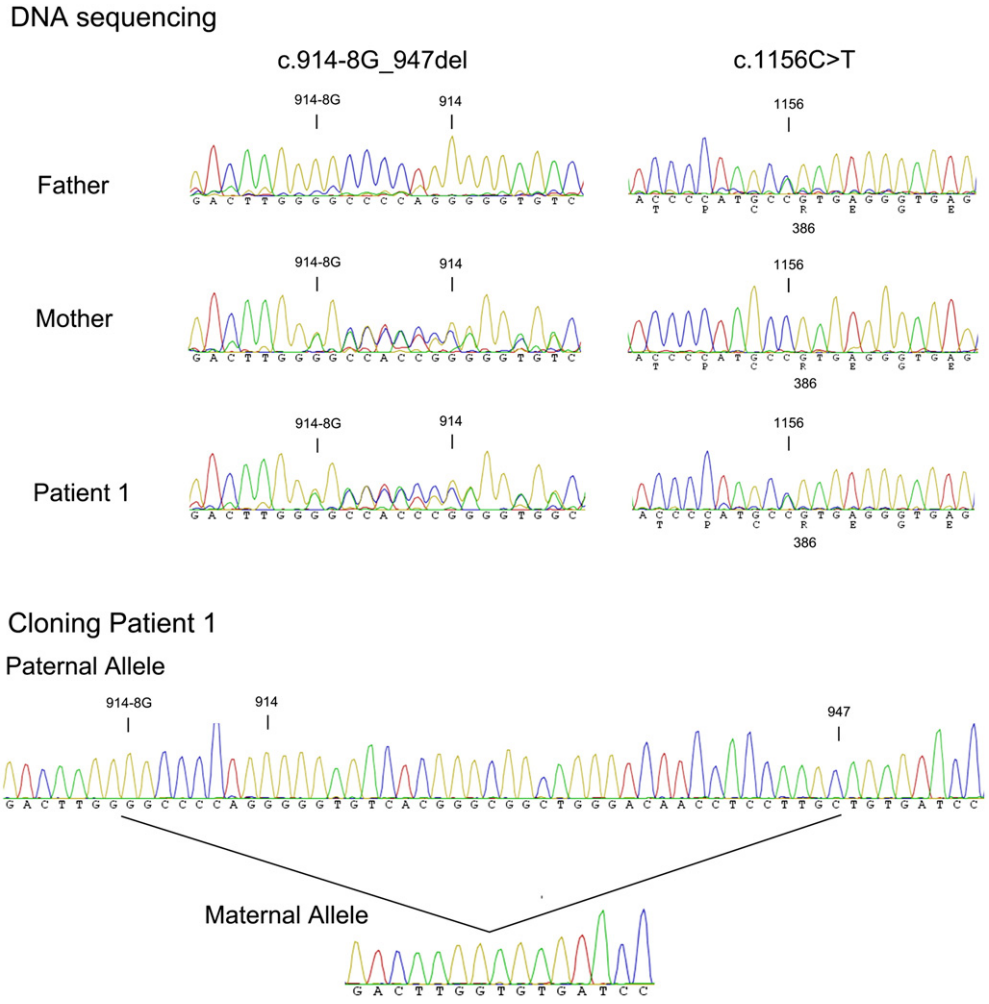

Fig. 3. Chromatograms displaying *NDUFV1* mutations. Top: direct sequencing of genomic *NDUFV1*-DNA from P1 and his parents. Bottom: direct sequencing of exons 6-7, previously cloned into a pCR4-TOPO-TA plasmid.

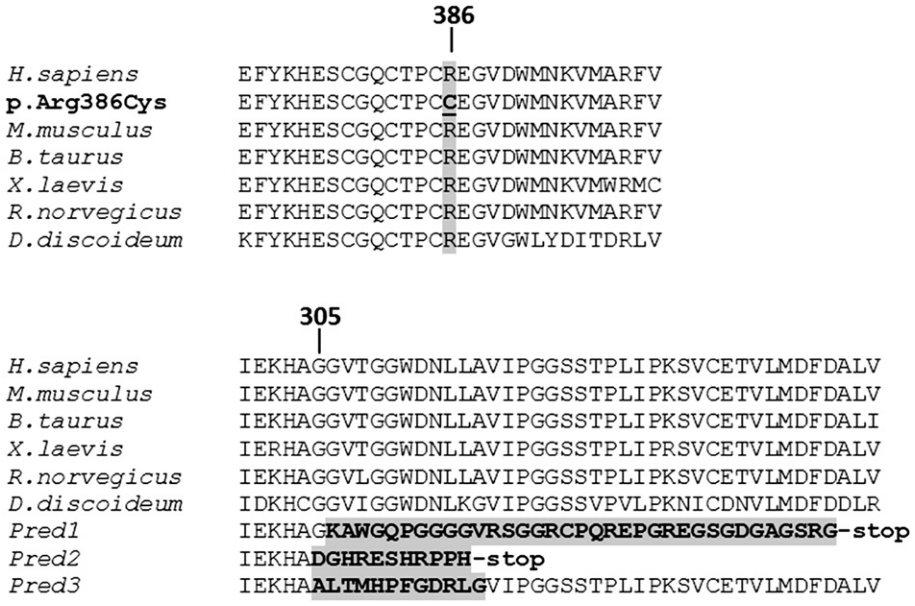

Fig. 4. Comparative sequence analysis of NDUFV1 orthologues. Top: Residues at position 386 are highlighted with gray shading. The p.Arg386Cys mutation is indicated in bold. Bottom: Aberrant protein tails generated by c.914-8G_947del mutation are highlighted with gray shading and indicated in bold. *Pred1*, *Pred2* and *Pred3* refer to distinct *in silico* predictions.

Table 1
Clinical and molecular features of patients presenting *NDUFV1* mutations.

Patient	Age of onset	Gender	Clinical presentation	Biochemical analysis	MRI	Mutation	Reference
1-2	5 months	M	Progressive muscular hypotonia, strabismus, myoclonic epilepsy psychomotor regression	Elevated lactate and piruvate concentrations in blood and CSF[a].	Brain Atrophy (CT-Scan)	c.1268C>T (p.T423M)/ c.175 C>T (p.R59X)	Schuelke et al., 1999
3	6 months	F	Infantile myoclonic epilepsy. Severe muscular hypotonia and macrocephaly	Elevated lactate in CSF but normal in blood and urine	Brain atrophy and progressive macrocystic leukodystrophy	c.1022 C>T (p.A341V)/ c.1022 C>T (p.A341V)	Schuelke et al., 1999
4	1 year	M	Seizures, cerebellar ataxia, psychomotor regression. Died at 3 years	Elevated lactate	Brain atrophy and multiple symmetric areas of hyperintensity in the brain stem	c.640G>A (p.E214K)/ c.1192+4A>C (Skipping of exon 8)	Benit et al., 2001
5	6 months	F	Recurrent episodes of vomiting, hypotonia, lethargy. She died at age of 18 months	Metabolic acidosis with high levels of lactate	Hyperintensity in the basal ganglia (T2)	c.990delTG/c.1294G>C (p.A432P)	Benit et al., 2001
6	5 months	M	Ptosis, strabismus, hypotonia, ataxia and ophtalmoplegia	Metabolic acidosis with high levels of lactate	Hyperintensity of the locus niger	c.611A>G (p.Y204C)/ c.616T>G (p.C206G)	Benit et al., 2001
7-8	First months	NR[b]	Progressive neurological disorder, involuntary movements. Signs of brainstem involvement	Lactic acidosis. Increased CSF lactate.	Diffuse leukoencephalopathy with large cavitations in the frontal and temporal subcortical white matter. Ventricular enlargement and macrocephaly.	c. 1022C>T (p.A341V)	Bugiani et al., 2004
9	6 months	NR	Psychomotor regression evolving into a spastic quadriparesis with loss of postural control	Lactic acidosis.	Diffuse leukoencephalopathy with no cavitations.	c.1564C>A (p.Q522K)	Bugiani et al., 2004
10	7 months	M	Progressive ophtalmoplegia, cerebellar ataxia, spasticity, dystonia	High levels of lactate in blood and CSF.	Bilateral hyperintensities in the putamen, red nuclei, and substantia nigrae (T2)	c.611A>G (p.Y204C)/ c.616T>G (p.C206G)	Laugel et al., 2007
11	6 months	F	Irritability, development regression	Normal lactate and piruvate concentrations in blood and CSF. Increased CSF lactate to pyruvate ratio.	Increased T2 and decreased T1 signal extending throughout the periventricular white matter to the subcortical white matter.	c.1155C>T (p.R386C)/ c.1155C>T (p.R386C)	Breningstall et al., 2008
12	11 months	M	Development regression	NR	Abnormal signal on the supratentorial matter, central areas of low signal on FLAIR images.	c.1155C>T (p.R386C)/ c.1155C>T (p.R386C)	Breningstall et al., 2008
13	9 months	F	Regression of motor milestones. Signs of mild spastic diplegia	Elevated lactate in blood.	Periventricular white matter abnormalities with sparing of the subcortical white matter.	c.632T>C (p.A211V)/ c.770G>A (p.R257Q)	Zafeiriou et al., 2008
14	NR	NR	Lethal infantile mitochondrial disease	NR	NR	c.1129G>A (p.E377K)	Calvo et al., 2010
15	14 months	M	Leukoencephalopathy and epilepsy	Metabolic acidosis	NR	(p.W51X)/(p.T423M)	Moran et al., 2010
16	3,5 months	M	Recurrent vomiting, failure to thrive. Hypotonia, irritability, nystagmus.	Lactate levels normal in blood and CSF	T2 Hypersignal in the posterior part of the medulla, the pons and the mesencephalon with normal basal ganglia.	c.1156G>A (p.R386H)	Vilain et al., 2012
17	3,5 months	F	Rotatory nistagmus, peripheral hypotonia.	Lactate midly elevated in serum and CSF	Symmetric T2 hypersignal in the pons and medulla.	c.1156G>A (p.R386H)	Vilain et al., 2012
18	8 months	M	Development regression, pyramidal signs, hypotonia and mild ataxia	NR	White signal abnormalities without involvement of the basal ganglia and brainstem.	(p.S56P)/(p.T423M)	Koene et al., 2012
19	1 year	M	Development regression, spasticity, brisk reflexes, strabismus and nystagmus	High levels of lactate in blood and CSF	Prominent signal abnormalities in large regions of the cerebral white matter, which include the corpus callosum	c.1156C>T (p.Arg386Cys)/ c.914-8G_947del	Present report
20	1 year	M	Psychomotor regression, weakness, spasticity.	Normal Lactate in blood and CSF	Prominent signal abnormalities in large regions of the cerebral white matter, which include the corpus callosum	c.1156C>T (p.Arg386Cys)/ c.914-8G_947del	Present report

[a] CSF: cerebrospinal fluid.
[b] CSF: non-reported.

reported by Schuelke et al. (1999) (p.Arg59X mutation), indicate that a single *NDUFV1* copy is sufficient to guarantee a CI minimal function.

6. Conclusions

Taken together, although our results do not permit to propose an accurate genotype–phenotype correlation, they add information on the molecular basis and the phenotypic features of mitochondrial disease caused by *NDUFV1* mutations. We can affirm that mutations presented here are causative of the phenotype. We hope that our results will encourage further researchers to explore, from a functional perspective, the molecular role of *NDUFV1* nonsense mutations.

Supplementary data to this article can be found online at http://dx.doi.org/10.1016/j.mito.2013.03.010.

Acknowledgments

We thank the patients and their family for their participation. This study was supported by The Universidad del Rosario (Grant CS/Genetics 2012).

References

Bateman, J.F., Freddi, S., Nattrass, G., Savarirayan, R., 2003. Tissue-specific RNA surveillance? Nonsense-mediated mRNA decay causes collagen X haploinsufficiency in Schmid metaphyseal chondrodysplasia cartilage. Hum. Mol. Genet. 12 (3), 217–225.

Benit, P., Chretien, D., Kadhom, N., de Lonlay-Debeney, P., Cormier-Daire, V., Cabral, A., Peudenier, S., Rustin, P., Munnich, A., Rotig, A., 2001. Large-scale deletion and point mutations of the nuclear NDUFV1 and NDUFS1 genes in mitochondrial complex I deficiency. Am. J. Hum. Genet. 68 (6), 1344–1352.

Brandt, U., 2006. Energy converting NADH:quinone oxidoreductase (complex I). Annu. Rev. Biochem. 75, 69–92.

Breningstall, G.N., Shoffner, J., Patterson, R.J., 2008. Siblings with leukoencephalopathy. Semin. Pediatr. Neurol. 15 (4), 212–215.

Brunak, S., Engelbrecht, J., Knudsen, S., 1991. Prediction of human mRNA donor and acceptor sites from the DNA sequence. J. Mol. Biol. 220 (1), 49–65.

Bugiani, M., Invernizzi, F., Alberio, S., Briem, E., Lamantea, E., Carrara, F., Moroni, I., Farina, L., Spada, M., Donati, M.A., Uziel, G., Zeviani, M., 2004. Clinical and molecular findings in children with complex I deficiency. Biochim. Biophys. Acta 1659 (2–3), 136–147.

Calvo, S.E., Tucker, E.J., Compton, A.G., Kirby, D.M., Crawford, G., Burtt, N.P., Rivas, M., Guiducci, C., Bruno, D.L., Goldberger, O.A., Redman, M.C., Wiltshire, E., Wilson, C.J., Altshuler, D., Gabriel, S.B., Daly, M.J., Thorburn, D.R., Mootha, V.K., 2010. High-throughput, pooled sequencing identifies mutations in NUBPL and FOXRED1 in human complex I deficiency. Nat. Genet. 42 (10), 851–858.

den Dunnen, J.T., Antonarakis, S.E., 2000. Mutation nomenclature extensions and suggestions to describe complex mutations: a discussion. Hum. Mutat. 15 (1), 7–12.

Hirst, J., Carroll, J., Fearnley, I.M., Shannon, R.J., Walker, J.E., 2003. The nuclear encoded subunits of complex I from bovine heart mitochondria. Biochim. Biophys. Acta 1604 (3), 135–150.

Janssen, R.J., Nijtmans, L.G., van den Heuvel, L.P., Smeitink, J.A., 2006. Mitochondrial complex I: structure, function and pathology. J. Inherit. Metab. Dis. 29 (4), 499–515.

Koene, S., Rodenburg, R.J., van der Knaap, M.S., Willemsen, M.A., Sperl, W., Laugel, V., Ostergaard, E., Tarnopolsky, M., Martin, M.A., Nesbitt, V., Fletcher, J., Edvardson, S., Procaccio, V., Slama, A., van den Heuvel, L.P., Smeitink, J.A., 2012. Natural disease course and genotype–phenotype correlations in Complex I deficiency caused by nuclear gene defects: what we learned from 130 cases. J. Inherit. Metab. Dis. 35 (5), 737–747.

Laugel, V., This-Bernd, V., Cormier-Daire, V., Speeg-Schatz, C., de Saint-Martin, A., Fischbach, M., 2007. Early-onset ophthalmoplegia in Leigh-like syndrome due to NDUFV1 mutations. Pediatr. Neurol. 36 (1), 54–57.

Lebre, A.S., Rio, M., Faivre d'Arcier, L., Vernerey, D., Landrieu, P., Slama, A., Jardel, C., Laforet, P., Rodriguez, D., Dorison, N., Galanaud, D., Chabrol, B., Paquis-Flucklinger, V., Grevent, D., Edvardson, S., Steffann, J., Funalot, B., Villeneuve, N., Valayannopoulos, V., de Lonlay, P., Desguerre, I., Brunelle, F., Bonnefont, J.P., Rotig, A., Munnich, A., Boddaert, N., 2011. A common pattern of brain MRI imaging in mitochondrial diseases with complex I deficiency. J. Med. Genet. 48 (1), 16–23.

Moran, M., Rivera, H., Sanchez-Arago, M., Blazquez, A., Merinero, B., Ugalde, C., Arenas, J., Cuezva, J.M., Martin, M.A., 2010. Mitochondrial bioenergetics and dynamics interplay in complex I-deficient fibroblasts. Biochim. Biophys. Acta 1802 (5), 443–453.

Nagy, E., Maquat, L.E., 1998. A rule for termination-codon position within intron-containing genes: when nonsense affects RNA abundance. Trends Biochem. Sci. 23 (6), 198–199.

Pagniez-Mammeri, H., Loublier, S., Legrand, A., Benit, P., Rustin, P., Slama, A., 2012. Mitochondrial complex I deficiency of nuclear origin I. Structural genes. Mol. Genet. Metab. 105 (2), 163–172.

Schuelke, M., Smeitink, J., Mariman, E., Loeffen, J., Plecko, B., Trijbels, F., Stockler-Ipsiroglu, S., van den Heuvel, L., 1999. Mutant NDUFV1 subunit of mitochondrial complex I causes leukodystrophy and myoclonic epilepsy. Nat. Genet. 21 (3), 260–261.

Skladal, D., Halliday, J., Thorburn, D.R., 2003. Minimum birth prevalence of mitochondrial respiratory chain disorders in children. Brain 126 (Pt 8), 1905–1912.

Stanke, M., Tzvetkova, A., Morgenstern, B., 2006. AUGUSTUS at EGASP: using EST, protein and genomic alignments for improved gene prediction in the human genome. Genome Biol. 7 (Suppl. 1), 11–18 (S11).

Thorburn, D.R., 2004. Mitochondrial disorders: prevalence, myths and advances. J. Inherit. Metab. Dis. 27 (3), 349–362.

Vilain, C., Rens, C., Aeby, A., Baleriaux, D., Van Bogaert, P., Remiche, G., Smet, J., Van Coster, R., Abramowicz, M., Pirson, I., 2012. A novel NDUFV1 gene mutation in complex I deficiency in consanguineous siblings with brainstem lesions and Leigh syndrome. Clin. Genet. 82 (3), 264–270.

Zafeiriou, D.I., Rodenburg, R.J., Scheffer, H., van den Heuvel, L.P., Pouwels, P.J., Ververi, A., Athanasiadou-Piperopoulou, F., van der Knaap, M.S., 2008. MR spectroscopy and serial magnetic resonance imaging in a patient with mitochondrial cystic leukoencephalopathy due to complex I deficiency and NDUFV1 mutations and mild clinical course. Neuropediatrics 39 (3), 172–175.